How Do Membrane Transporters Sense pH? The Case of the Mitochondrial ADP–ATP Carrier

ARTICLE *in* JOURNAL OF PHYSICAL CHEMISTRY LETTERS · OCTOBER 2013

Impact Factor: 7.46 · DOI: 10.1021/jz401847d

7 AUTHORS, INCLUDING:

Eva-Maria Krammer

Université des Sciences et Technologies de Lill…

23 PUBLICATIONS **190** CITATIONS

SEE PROFILE

Chris Chipot

French National Centre for Scientific Research…

163 PUBLICATIONS **11,813** CITATIONS

SEE PROFILE

THE JOURNAL OF PHYSICAL CHEMISTRY Letters

Letter

pubs.acs.org/JPCL

How Do Membrane Transporters Sense pH? The Case of the Mitochondrial ADP–ATP Carrier

Axel Bidon-Chanal,[†,‡,▽] Eva-Maria Krammer,[†,‡,▽] Delphine Blot,[§,⊥,#] Eva Pebay-Peyroula,[§,⊥,#] Christophe Chipot,[†,‡,∥] Stéphanie Ravaud,*[,§,⊥,#] and François Dehez*[,†,‡,∥]

[†]Université de Lorraine, BP 239, 54506 Vandoeuvre-lès-Nancy Cedex, France

[‡]CNRS, UMR 7565 SRSMC, 54506 Vandoeuvre-lès-Nancy, France

[§]Univ. Grenoble Alpes, Institut de Biologie Structurale (IBS), 6 rue Jules Horowitz -38000 Grenoble, France

[⊥]CEA, DSV, IBS, 38000 Grenoble, France

[#]CNRS, IBS, 38000 Grenoble, France

[∥]Laboratoire International Associé CNRS/ University of Illinois at Urbana–Champaign, 54506 Vandoeuvre-les-Nancy, France

Supporting Information

ABSTRACT: The activity of many membrane proteins depends markedly on the pH. Pinpointing the amino acids forming the pH sensor domains of these proteins remains challenging for current experimental techniques. Combining molecular dynamics simulations and pK_a predictions with in vitro transport assays, we have revealed the molecular basis of the pH dependence of the mitochondrial carrier mediating the exchanges of ADP^{3-} and ATP^{4-} across the inner mitochondrial membrane. We have demonstrated that the transport activity of this mitochondrial carrier depends on the protonation state of both the substrate and a unique, highly conserved residue of the protein. The original strategy proposed here offers a convenient framework for identifying pH-sensitive residues in membrane proteins in such cases where one single amino acid is involved. Our findings are envisioned to help toward the rational design of active compounds ranging from drugs to biosensors.

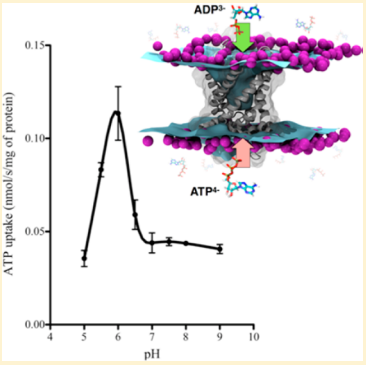

SECTION: Biophysical Chemistry and Biomolecules

The question of the protonation state of titratable residues in membrane proteins and their connection to the function of the latter remains a daunting challenge for membrane proteins.[1,2] Recent studies have attempted to identify key residues in specific membrane proteins, the function of which depends upon the protonation state of the former and, hence, upon the pH.[3−5] Such studies can, however, only determine indirectly the regions of the protein that sense pH, but only rarely are individual residues in these regions determined. From a theoretical perspective, pinpointing pH-sensitive residues in membrane proteins represents an equal challenge, as attested to by the recent literature.[6−8] In the latter computational investigations, the identity of the titratable residues is known beforehand, and these residues are examined using a variety of methods ranging from a molecular mechanical to a quantum chemical treatment of a fragment of the membrane protein. The difficulties that these studies have brought to light emphasized the necessity for novel strategies. Here, we combined molecular dynamics simulations and pK_a predictions with in vitro transport assays to reveal the molecular basis of the pH dependence of the mitochondrial carrier mediating the exchanges of ADP^{3-} and ATP^{4-} across the inner mitochondrial membrane.

ATP^{4-}, the energy fuel of the cell, is synthesized from ADP^{3-} in the mitochondrial matrix. Optimal energetic balance in the cell requires continuous exchange of ATP^{4-} and ADP^{3-} across the inner mitochondrial membrane, alteration of this process leading to a variety of pathologies.[9−11] Transport of ADP^{3-} and ATP^{4-} is mediated by the highly substrate-specific ADP/ATP carrier (AAC), a member of the mitochondrial carrier family.[12−15] Due to its abundance in heart mitochondria, the AAC is the best-characterized mitochondrial carrier[16] and, to this date, the only one for which high-resolution structural data are available.[17,18] The structure, solved in the presence of the inhibitor carboxyatractyloside, reveals six transmembrane α-helical segments forming a compact bundle of pseudo-3-fold symmetry. The inhibitor occupies a deep internal cavity, occluded on the matrix side and wide open toward the intermembrane space. It was shown that conformational flexibility of the protein is a key element of the transport process.[10,19−21] Two patches of basic residues line this cavity. The upper basic patch is located at the mouth of AAC, and the lower one delineates the bottom of the cavity. These two

Received: August 30, 2013
Accepted: October 15, 2013
Published: October 15, 2013

   dx.doi.org/10.1021/jz401847d | J. Phys. Chem. Lett. 2013, 4, 3787−3791

patches are responsible for the unique electrostatic signature of the AAC, its funnel-shaped three-dimensional electrostatic potential driving rapidly the substrate down toward the bottom of the internal cavity.[22,23] Mutation or screening of the latter basic residues by high salt concentrations abolishes the transport activity of the AAC.[24,25] The AAC function has also been described to be pH-dependent. Using capacitive-current measurements combined with caged ATP^{4-} and ADP^{3-} photolysis in reconstituted liposomes, Broustovetsky et al. showed that ADP^{3-}/ATP^{4-} exchange is maximal at pHs lying between 6.5 and 7.5.[26] These authors attributed the origin of the pH dependence chiefly to the protonation state of the substrate while suggesting a possible implication of one or several basic amino acids of the AAC. In the present study, we combine synergistically experimental and theoretical approaches to demonstrate that the AAC activity depends not only on the protonation state of the substrate but also on that of the protein. Our investigation reveals the identity of a single, highly conserved amino acid, responsible for the pH dependence of ADP^{3-}/ATP^{4-} transport across the inner membrane of mitochondria.

Transport activity assays of [α-^{32}P]-labeled ATP^{4-} by the isoform 1 of human AAC (hAAC1) expressed in *E. coli* (see Supporting Information section 1) were carried out to follow the variation of the protein activity over a wide range of pH values (Figure 1). Our results agree with the pH dependence curves reported by Broustovetsky et al. for ADP^{3-} (see Figure 9 of ref 26). Protein activity is found to be optimal at a pH between 6 and 7.5, as a function of the experimental setup. The pH of the intermembrane space is about 6.9,[27] and the pK_a's of

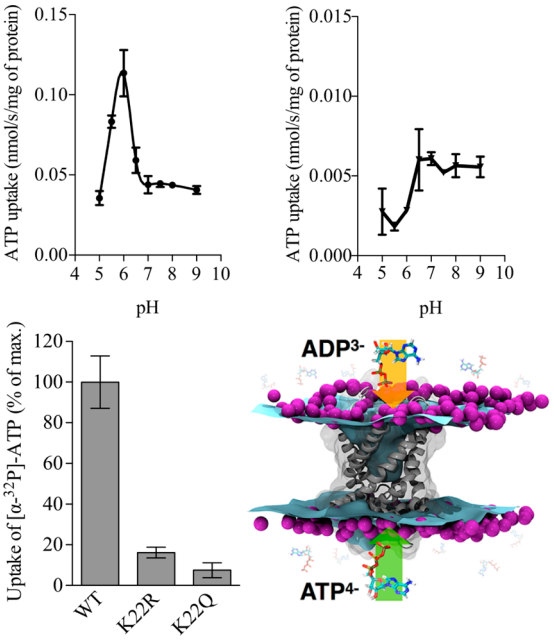

Figure 1. (Top left) pH dependence of [α-^{32}P]-ATP uptake into *E. coli* cells expressing hAAC1. (Top right) pH dependence of [α-^{32}P]-ATP uptake into *E. coli* cells expressing K22R mutant of hAAC1. (Bottom left) Transport activities of K22R and K22Q mutants compared to the wild-type. For clarity, the bovine heart AAC1 sequence numbering was systematically adopted; in hAAC, K22 corresponds to K23. (Bottom right) Schematic illustration of ADP^{3-}/ATP^{4-} exchange through the AAC. Violet spheres represent phospholipid head groups, and the ice-blue surface is an isocontour of the electrostatic potential.

ADP^{3-} and ATP^{4-} are equal to 6.3 and 6.7, respectively. At low pH, impairment of the substrate transport is rooted in the increase of the concentration of the protonated nucleotides, at the expense of their deprotonated counterparts, the latter being the only species transported by the AAC.[14] At high pH values, the substrates primarily exist in their deprotoned form, that is, ADP^{3-} and ATP^{4-}. Decrease of transport activity, therefore, cannot be rationalized by the sole titration state of the nucleotides but is likely to depend also on the protonation state of one or several amino acids of the protein.

To identify residues of the protein that can possibly sense the variation of the pH in a range nearing that of the maximum activity of the carrier, we systematically estimated the pK_a of all titratable residues of the protein with the PROPKA v3.1 software.[28,29] Although it is clear that pK_a prediction algorithms have not yet demonstrated unequivocally their robustness to be considered fully predictive, they, nonetheless, provide a guiding hand to help design experiments that will either confirm or disprove working hypotheses. The calculations were run over 500 representative conformations extracted from the 100 ns molecular dynamics trajectory generated with the apo wild-type bovine heart AAC embedded in a fully hydrated POPC bilayer (Figure 2) (see Supporting Information sections 2 and 3).

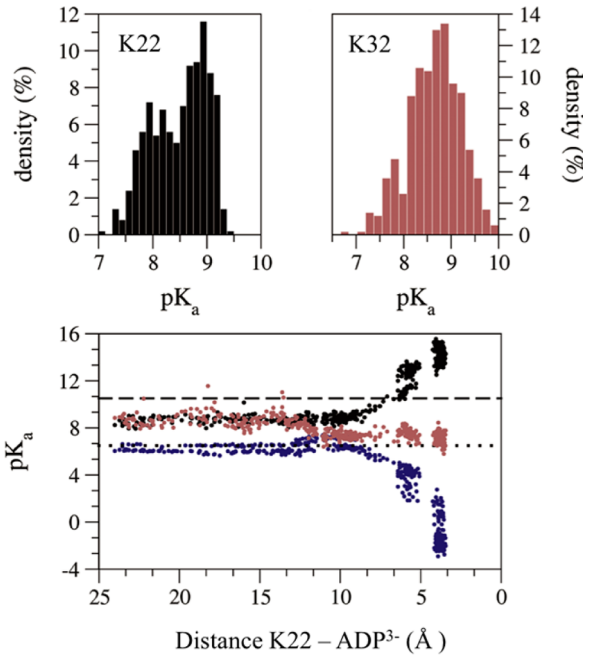

Figure 2. pK_a distributions computed with PROPKA over the last 50 ns of simulation of the apo wild-type AAC for the amino group in the side chains of K22 (top left) and K32 (top right). (Bottom) pK_a evolution of K22 (black dots) and K32 (brown dots) and ADP^{3-} (blue dots) as a function of the distance between the substrate and K22. The dashed and the dotted lines represent the experimental estimates of the pK_a of lysine and ADP^{3-} in aqueous solution.

From this exhaustive study, only two residues emerged, K22 and K32, exhibiting unusually low pK_a values, 8.5 ± 0.5 and 8.6 ± 0.6, respectively (Figure 2), suggestive of a sensitivity to the pH near the optimal value for AAC activity. Although both residues are located in the same region of the AAC, K32 is buried at the bottom of the internal cavity, its side chain forming long-lived interactions with the side chain of Q36 and D231, whereas K22 lies in the middle of the cavity, its side

dx.doi.org/10.1021/jz401847d | J. Phys. Chem. Lett. 2013, 4, 3787−3791

chain not being engaged in any interaction with neighboring residues. On its way down to the binding site, ADP^{3-} establishes several interactions with the side chains lining the cavity of the protein, including K22 but not K32 (Figure 3).

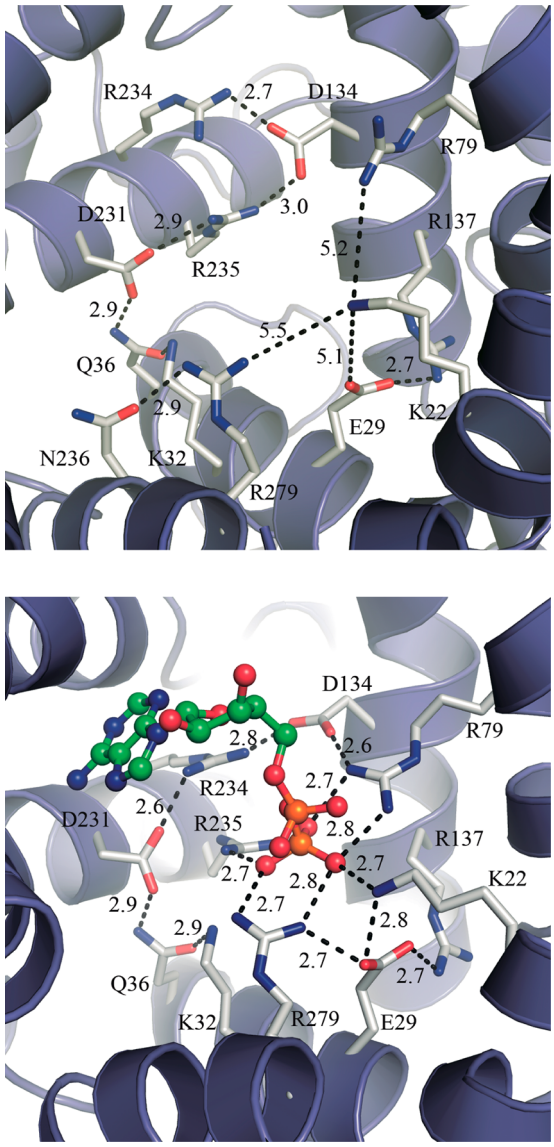

Figure 3. (Top) Close view of the residues surrounding K22 in the apo wild-type protein. (Bottom) Close view of the ADP^{3-} putative binding motif based on an all-atom simulation of AAC in the presence of the nucleotide. All reported distances are given in Å.

Lower pK_a values of 6.0 ± 0.6 and 6.5 ± 0.5 were inferred for K22 using, respectively, H++[30] and QMBP/GMCT,[31−33] methods aimed at predicting the protonation probabilities of titratable residues (see Supporting Information Figure 1). These approaches consistently indicate that the buried K32 cannot be deprotoned (see Supporting Information section 3). It should be stressed that our results do not depend on the protonation state assumed during the MD simulation (see Supporting Information Figure 2). Interestingly enough, the pK_a of ADP^{3-} and K22 (albeit not that of K32) varies as a function of the distance separating the nucleotide from the bottom of the protein cavity (see Figure 2). When the complex is steadily formed, ADP^{3-} and K22 are, respectively, deprotonated and protonated over a wide range of pH values. Put together, our data strongly suggest that K22 is involved in the dependence of AAC transport activity to the pH.

Numerical association assays (see Supporting Information section 1) were carried out to rationalize the effect of the pH on the binding of ADP^{3-} to the carrier. Three different assemblies were constructed, namely, protonated K22/protonated nucleotide ($ADPH^{2-}$), protonated K22/deprotonated nucleotide (ADP^{3-}), and deprotonated K22/deprotonated nucleotide (ADP^{3-}), reflecting acidic, physiological, and basic conditions, respectively. For each assembly, 100 ns molecular dynamics simulations starting from five different orientations of the substrate positioned at the mouth of the carrier were carried out.

Under physiological conditions, ADP^{3-} reached its binding site four times out of five within 25 ns. Going down the internal cavity, ADP^{3-} formed transient contacts with the upper basic patch, as described earlier.[22−24] In sharp contrast, binding was never observed for basic conditions and was monitored only two times for acidic ones, on the 100 ns time scale. In basic conditions, deprotonation of K22 lowered the total charge at the bottom of the cavity and, hence, modified the topology of the electrostatic field inside of the AAC. Such an alteration has been shown to impair systematically the transport activity of the carrier.[10,25] Furthermore, point mutation of K22 into alanine was demonstrated to abolish the activity of the protein.[13] In acidic conditions, the effect of protonation of ADP^{3-} on binding is not as clear-cut.

Using the adaptive biasing force algorithm[34,35] implemented in the NAMD package,[36] we generated two one-dimensional potentials of mean force (PMFs) measuring the reversible work required to translocate the nucleotide from the mouth of the carrier to the bottom of its internal cavity, in physiological and basic pH conditions (see Supporting Information section 4). The two PMFs depicted in Figure 4 ought to be seen as mere indicators of the affinity of the two nucleotides, ADP^{3-} and $ADPH^{2-}$, toward the internal cavity of the AAC. All things being equal, recognition of the deprotonated form of the substrate is to be far more favorable than that of its protonated counterpart. Maintaining the total charge of the endogenous substrates of the AAC, therefore, appears to be as important as preserving the native electrostatic signature of the protein to ensure optimal transport activity.

Uptake assays were performed for two mutants, namely, K22Q and K22R (in the hAAC1 sequence, K22 corresponds to K23). Mutating K22 into glutamine abolishes transport activity (Figure 1), emphasizing the importance of preserving the net charge of the internal cavity to guarantee the function of the protein. In contrast, the carrier activity, however markedly lowered, remained measurable upon mutation of K22 into arginine, the pK_a of the latter residue being unaffected by the cavity environment (see Supporting Information Figure 3). pH dependence experiments were carried out for K22R (Figure 1) and compared to the results obtained for the wild-type hAAC1. For both the wild-type and the mutant, the transport activity diminished when going from physiological to acidic conditions as a result of the increase of nontransportable protonated substrates, $ADPH^{2-}$. In the case of K22R, increasing the pH from physiological to basic conditions did not alter transport; the activity rather plateaus around a maximum value, in glaring contrast with the wild-type. The striking difference in the shape of the two pH dependence profiles cogently demonstrates the direct implication of K22 in the pH-sensing ability of hAAC1.

dx.doi.org/10.1021/jz401847d | J. Phys. Chem. Lett. 2013, 4, 3787−3791

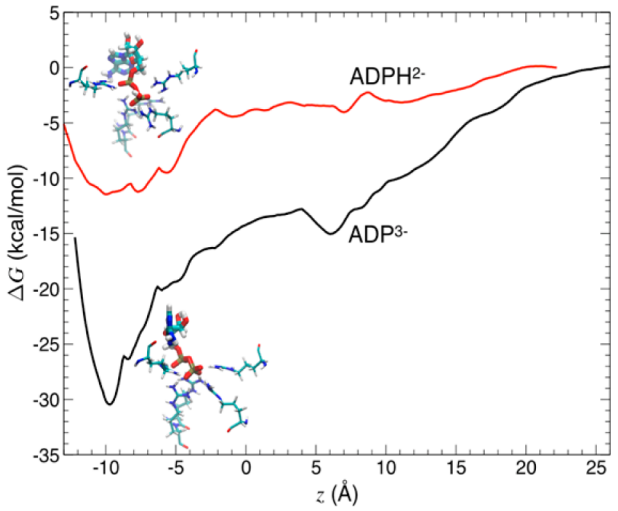

Figure 4. One-dimensional PMFs delineating the reversible association of ADP^{3-} (black curve) and $ADPH^{2-}$ (red curve) to the internal cavity of the AAC with protonated K22. The free-energy differences were determined using the adapting biasing force method. z corresponds to the Euclidian distance separating the last phosphate moiety of the nucleotides from the center of mass of the transmembrane helices, projected onto the longitudinal axis of the carrier. The total simulation times needed for mapping the free-energy landscapes of ADP^{3-} and $ADPH^{2-}$ binding the AAC amount to 624 and 580 ns, respectively.

To summarize, the present data reveal that the transport activity of AAC does not only depend on the protonation state of the substrate but also on that of the protein. Combining theoretical and experimental assays, we have shown that a single residue, K22, highly conserved in all AAC sequences, allows the protein to sense pH variations. By virtue of a pK_a value much lower than that expected in the bulk environment, this lysine residue is mainly deprotonated in basic conditions, a situation conducive to impair severely AAC activity. At variance, mutating K22 into arginine caused the knockout of the protein response to basic conditions. The original strategy put forth herein is envisioned to help in pinpointing amino acids composing pH sensor domains of membrane proteins.

■ ASSOCIATED CONTENT

Supporting Information

Experimental protocols and methodological details, including transport activity measurements, molecular dynamics simulations, pK_a calculations, and potential of mean force details, are given. This material is available free of charge via the Internet at http://pubs.acs.org.

■ AUTHOR INFORMATION

Corresponding Authors

*E-mail: Stephanie.Ravaud@ibs.fr (S.R.).

*E-mail: François.Dehez@univ-lorraine.fr (F.D.).

Author Contributions

▽A.B.-C. and E.-M.K. contributed equally.

Notes

The authors declare no competing financial interest.

■ ACKNOWLEDGMENTS

This work was supported by the Agence National de La Recherche (ANR MIT-2M, N°ANR 2010 BLAN1518-01) and the Direction Régionale à la Recherche et à la Technologie de Lorraine. The Grand Equipement National de Calcul Informatique (GENCI) and the Centre Informatique National de l'Enseignement Supérieur (CINES) are gratefully acknowledged for the provision of computer time.

■ REFERENCES

(1) Frericks Schmidt, H. L.; Shah, G. J.; Sperling, L. J.; Rienstra, C. M. NMR Determination of Protein pK_a Values in the Solid State. *J. Phys. Chem. Lett.* **2010**, *1*, 1623−1628.

(2) Gleason, N. J.; Vostrikov, V. V.; Greathouse, D. V.; Koeppe, R. E. Buried Lysine, But Not Arginine, Titrates and Alters Transmembrane Helix Tilt. *Proc. Natl. Acad. Sci. U.S.A.* **2013**, *110*, 1692−1695.

(3) Thompson, A. N.; Posson, D. J.; Parsa, P. V.; Nimigean, C. M. Molecular Mechanism of pH Sensing in KcsA Potassium Channels. *Proc. Natl. Acad. Sci. U.S.A.* **2008**, *105*, 6900−6905.

(4) Hu, F.; Schmidt-Rohr, K.; Hong, M. NMR Detection of pH-Dependent Histidine−Water Proton Exchange Reveals the Conduction Mechanism of a Transmembrane Proton Channel. *J. Am. Chem. Soc.* **2012**, *134*, 3703−3713.

(5) Hong, M.; DeGrado, W. F. Structural Basis for Proton Conduction and Inhibition by the Influenza M2 Protein. *Protein Sci.* **2012**, *21*, 1620−1633.

(6) Li, L.; Vorobyov, I.; Allen, T. W. Potential of Mean Force and pK_a Profile Calculation for a Lipid Membrane-Exposed Arginine Side Chain. *J. Phys. Chem. B* **2008**, *112*, 9574−9587.

(7) Goyal, P.; Ghosh, N.; Phatak, P.; Clemens, M.; Gaus, M.; Elstner, M.; Cui, Q. Proton Storage Site in Bacteriorhodopsin: New Insights from Quantum Mechanics/Molecular Mechanics Simulations of Microscopic pK_a and Infrared Spectra. *J. Am. Chem. Soc.* **2011**, *133*, 14981−14997.

(8) Zhu, S.; Brown, M. F.; Feller, S. E. Retinal Conformation Governs pK_a of Protonated Schiff Base in Rhodopsin Activation. *J. Am. Chem. Soc.* **2013**, *135*, 9391−9398.

(9) Palmieri, F. Diseases Caused by Defects of Mitochondrial Carriers: A Review. *Biochim. Biophys. Acta, Bioenerg.* **2008**, *1777*, 564−578.

(10) Ravaud, S.; Bidon-Chanal, A.; Blesneac, I.; Machillot, P.; Juillan-Binard, C.; Dehez, F.; Chipot, C.; Pebay-Peyroula, E. Impaired Transport of Nucleotides in a Mitochondrial Carrier Explains Severe Human Genetic Diseases. *ACS Chem. Biol.* **2012**, *7*, 1164−1169.

(11) Clémençon, B.; Babot, M.; Trézéguet, V. The Mitochondrial ADP/ATP Carrier (SLC25 Family): Pathological Implications of Its Dysfunction. *Mol. Aspects Med.* **2013**, *34*, 485−493.

(12) Kunji, E. R. The Role and Structure of Mitochondrial Carriers. *FEBS Lett.* **2004**, *564*, 239−244.

(13) Nury, H.; Dahout-Gonzalez, C.; Trézéguet, V.; Lauquin, G. J. M.; Brandolin, G.; Pebay-Peyroula, E. Relations Between Structure and Function of the Mitochondrial ADP/ATP Carrier. *Annu. Rev. Biochem.* **2006**, *75*, 713−741.

(14) Mifsud, J.; Ravaud, S.; Krammer, E.-M.; Chipot, C.; Kunji, E. R. S.; Pebay-Peyroula, E.; Dehez, F. The Substrate Specificity of the Human ADP/ATP Carrier AAC1. *Mol. Membr. Biol.* **2013**, *30*, 160−168.

(15) Monné, M.; Palmieri, F.; Kunji, E. R. S. The Substrate Specificity of Mitochondrial Carriers: Mutagenesis Revisited. *Mol. Membr. Biol.* **2013**, *30*, 149−159.

(16) Klingenberg, M. The ADP and ATP Transport in Mitochondria and Its Carrier. *Biochim. Biophys. Acta* **2008**, *1778*, 1978−2021.

(17) Pebay-Peyroula, E.; Dahout-Gonzalez, C.; Kahn, R.; Trézéguet, V.; Lauquin, G. J.-M.; Brandolin, G. Structure of Mitochondrial ADP/ATP Carrier in Complex with Carboxyatractyloside. *Nature* **2003**, *426*, 39−44.

(18) Nury, H.; Dahout-Gonzalez, C.; Trézéguet, V.; Lauquin, G.; Brandolin, G.; Pebay-Peyroula, E. Structural Basis for Lipid-Mediated Interactions Between Mitochondrial ADP/ATP Carrier Monomers. *FEBS Lett.* **2005**, *579*, 6031−6036.

(19) Johnston, J. M.; Khalid, S.; Sansom, M. S. P. Conformational Dynamics of the Mitochondrial ADP/ATP Carrier: A Simulation Study. *Mol. Membr. Biol.* **2008**, *25*, 506−517.
(20) Babot, M.; Blancard, C.; Pelosi, L.; Lauquin, G. J.-M.; Trézéguet, V. The Transmembrane Prolines of the Mitochondrial ADP/ATP Carrier Are Involved in Nucleotide Binding and Transport and Its Biogenesis. *J. Biol. Chem.* **2012**, *287*, 10368−10378.
(21) Babot, M.; Blancard, C.; Zeman, I.; Lauquin, G. J.-M.; Trézéguet, V. Mitochondrial ADP/ATP Carrier: Preventing Conformational Changes by Point Mutations Inactivates Nucleotide Transport Activity. *Biochemistry (Moscow)* **2012**, *51*, 7348−7356.
(22) Wang, Y.; Tajkhorshid, E. Electrostatic Funneling of Substrate in Mitochondrial Inner Membrane Carriers. *Proc. Natl. Acad. Sci. U.S.A.* **2008**, *105*, 9598−9603.
(23) Dehez, F.; Pebay-Peyroula, E.; Chipot, C. Binding of ADP in the Mitochondrial ADP/ATP Carrier Is Driven by an Electrostatic Funnel. *J. Am. Chem. Soc.* **2008**, *130*, 12725−12733.
(24) Krämer, R.; Kürzinger, G. The Reconstituted ADP/ATP Carrier from Mitochondria Is Both Inhibited and Activated by Anions. *Biochim. Biophys. Acta., Bioenerg.* **1984**, *765*, 353−362.
(25) Krammer, E.-M.; Ravaud, S.; Dehez, F.; Frelet-Barrand, A.; Pebay-Peyroula, E.; Chipot, C. High-Chloride Concentrations Abolish the Binding of Adenine Nucleotides in the Mitochondrial ADP/ATP Carrier Family. *Biophys. J.* **2009**, *97*, L25−L27.
(26) Broustovetsky, N.; Bamberg, E.; Gropp, T.; Klingenberg, M. Biochemical and Physical Parameters of the Electrical Currents Measured with the ADP/ATP Carrier by Photolysis of Caged ADP and ATP. *Biochemistry (Moscow)* **1997**, *36*, 13865−13872.
(27) Porcelli, A. M.; Ghelli, A.; Zanna, C.; Pinton, P.; Rizzuto, R.; Rugolo, M. pH Difference Across the Outer Mitochondrial Membrane Measured with a Green Fluorescent Protein Mutant. *Biochem. Biophys. Res. Commun.* **2005**, *326*, 799−804.
(28) Li, H.; Robertson, A. D.; Jensen, J. H. Very Fast Empirical Prediction and Rationalization of Protein pK_a Values. *Proteins: Struct., Funct., Bioinform.* **2005**, *61*, 704−721.
(29) Bas, D. C.; Rogers, D. M.; Jensen, J. H. Very Fast Prediction and Rationalization of pK_a Values for Protein−Ligand Complexes. *Proteins* **2008**, *73*, 765−783.
(30) Gordon, J. C.; Myers, J. B.; Folta, T.; Shoja, V.; Heath, L. S.; Onufriev, A. H++: A Server for Estimating pK_as and Adding Missing Hydrogens to Macromolecules. *Nucleic Acids Res.* **2005**, *33*, W368−W371.
(31) Ullmann, R. T.; Ullmann, G. M. Coupling of Protonation, Reduction, and Conformational Change in Azurin from Pseudomonas Aeruginosa Investigated with Free Energy Measures of Cooperativity. *J. Phys. Chem. B* **2011**, *115*, 10346−10359.
(32) Ullmann, R. T.; Andrade, S. L. A.; Ullmann, G. M. Thermodynamics of Transport Through the Ammonium Transporter Amt-1 Investigated with Free Energy Calculations. *J. Phys. Chem. B* **2012**, *116*, 9690−9703.
(33) Ullmann, R. T.; Ullmann, G. M. GMCT: A Monte Carlo Simulation Package for Macromolecular Receptors. *J. Comput. Chem.* **2012**, *33*, 887−900.
(34) Darve, E.; Pohorille, A. Calculating Free Energies Using Average Force. *J. Chem. Phys.* **2001**, *115*, 9169−9183.
(35) Hénin, J.; Chipot, C. Overcoming Free Energy Barriers Using Unconstrained Molecular Dynamics Simulations. *J. Chem. Phys.* **2004**, *121*, 2904−2914.
(36) Phillips, J. C.; Braun, R.; Wang, W.; Gumbart, J.; Tajkhorshid, E.; Villa, E.; Chipot, C.; Skeel, R. D.; Kalé, L.; Schulten, K. Scalable Molecular Dynamics with NAMD. *J. Comput. Chem.* **2005**, *26*, 1781−1802.